Simultaneous stress and birefringence measurements during uniaxial elongation of polystyrene melts with narrow molecular weight distribution

Author(s):
Luap, Clarisse; Müller, Christian; Schweizer, Thomas; Venerus, David C.

Publication date:
2005-09

Permanent link:
https://doi.org/10.3929/ethz-b-000031569

Originally published in:
Rheologica Acta 45(1), https://doi.org/10.1007/s00397-005-0452-5

Rheol Acta (2005) 45: 83–91
DOI 10.1007/s00397-005-0452-5

ORIGINAL CONTRIBUTION

Clarisse Luap
Christian Müller
Thomas Schweizer
David C. Venerus

Simultaneous stress and birefringence measurements during uniaxial elongation of polystyrene melts with narrow molecular weight distribution

Received: 6 October 2004
Accepted: 15 February 2005
Published online: 5 July 2005

C. Luap (✉) · C. Müller
T. Schweizer · D. C. Venerus
Department of Materials, ETH Zürich,
8093 Zürich, Switzerland
E-mail: Clarisse.Luap@mat.ethz.ch
Tel.: +41-1-632-68-89
Fax: +41-1-632-1076

D. C. Venerus
Department of Chemical and
Environmental Engineering and Center of
Excellence in Polymer Science and
Engineering, Illinois Institute of
Technology, Chicago, IL 60616, USA

Abstract Tensile stress and flow-induced birefringence have been measured during uniaxial elongation at a constant strain rate of two polystyrene melts with narrow molecular weight distribution. For both melts, the stress- optical rule (SOR) is found to be fulfilled upto a critical stress of 2.7 MPa, independent of strain rate and temperature. Estimation of the Rouse times of the melts, from both the zero-shear viscosity and the dynamic-shear moduli at high frequency, shows that the violation of the SOR occurs when the strain rate multiplied by the Rouse time of the melt exceeds by approximately 3. The presented results indicate that in contrast to current predictions of molecular theories, the regime of extensional thinning observed by Bach et al. (2003) extends well beyond the onset of failure of the SOR, and therefore the onset of chain stretch in the non-Gaussian regime.

Keywords Polymer melt · Birefringence · Elongational flow · Polystyrene · Rheo-optics · Nonlinear viscoelasticity

Introduction

Flows encountered during polymer processing can involve extremely large velocity gradients. To describe properties of entangled polymer melts in these fast flow situations, reptation-based molecular theories include the concept of chain stretch. Allowing chain retraction to be incomplete, the occupied tube length can exceed its equilibrium value. The retraction process is assumed to take place on a time scale given by the Rouse time τ_R of the chain, and therefore chain stretch can occur when the velocity gradient exceeds $1/\tau_R$. First introduced by Marrucci and Grizzuti (1988) into the original reptation model, the significance of the chain stretch mechanism is now well established as it explains two main particularities of the transient response of polymers upon start-up of fast steady flow: the appearance of an overshoot in the first normal stress difference in shear, and the phenomenon of strain hardening observed in elongational flow.

Concerning steady-state properties, current reptation-based theories predict that the onset of significant chain stretch gives rise to an upturn of the steady elongational viscosity at a strain rate of the order of the reciprocal Rouse time of the chain. At larger rates, provided that chain finite extensibility is taken into account, the viscosity grows with strain rate until it saturates when chains reach their full extension (Marrucci et al. 2004). While the predicted upturn of the elongational viscosity was confirmed experimentally for monodisperse entangled PS solutions (Bhattacharjee et al. 2002; Ye et al. 2003), the situation for melts is unclear. Early data by Li (1988) (see also Takahashi et al. 1993) on a polystyrene (PS) melt with a relatively

narrow molecular weight distribution (NMWD) indicated the onset of an extension thickening regime, though this conclusion relies on a single data point. The recent data on two PS melts with NMWD published by Bach et al. (2003) show, however, that the steady-state elongational viscosity decreases monotonically with the strain rate without any sign of an upturn in the vicinity of $\dot{\varepsilon}\tau_R \approx 1$. Though their transient data presented a substantial strain hardening, the lack of additional information about the degree of chain stretch apparently led to ambiguities in possible explanations. Whereas Bach et al. discussed the high rate scaling of the viscosity considering that chains nearly reach full extension, Marrucci and Ianniruberto (2004) suggested that the absence of upturn might be explained by an overestimation of the Rouse time of the melts. According to the latter argument, the onset of significant steady chain stretch and the resulting upturn in viscosity would occur simply at a higher strain rate, beyond the experimentally explored range.

Yet another experimental manifestation of strong chain stretching is the failure of the stress-optical rule (SOR) that occurs at large deformation when melts are stretched far above the glass transition temperature. The stress-optical rule states that the anisotropic parts of the refractive index and the stress tensors are proportional to each other. For uniaxial elongational flow it means that the birefringence Δn is related to the tensile stress σ through a constant stress-optical coefficient C, i.e., $\Delta n = C\ \sigma$. If chains stretch and approach their full extension, the SOR obviously fails since the stress continues to grow whereas the birefringence tends to saturate. More precisely, departure from the linear relation will occur when the degree of chain stretch is such that significant non-Gaussian effects set in (Mead and Leal 1995). For melts, such failure has been observed many times for uniaxial elongational flow (Matsumoto and Bogue 1977; Muller and Froelich 1985; Muller and Pesce 1994; Venerus et al. 1999). These studies concerned polydisperse systems only, and, to our knowledge, the unique stress-optical data published on a PS melt with a NMWD (Kotaka et al. 1997) reported violations from the SOR that are inconsistent with the occurrence of chain stretch beyond the Gaussian regime. It therefore remains unclear, above which stress level the degree of chain stretch is such that effect of finite extensibility becomes measurable, and above which stress level chains reach their full extension.

The goal of this study is to fill this lack of stress-optical data on PS melts with NMWD. We report simultaneous measurements of tensile stress and birefringence during the uniaxial elongation of two nearly monodisperse PS melts with molecular weights comparable to those used by Bach et al. (2003). Tests were performed within a temperature-strain rate suitable to evidence the breakdown of the SOR. We will show in particular that the regime of extensional thinning, observed by Bach et al. (2003), extends well beyond the onset of failure of the SOR and therefore the onset of significant chain stretch in the non-Gaussian regime.

Experimental details

Materials and samples preparation

Two anionic polystyrenes with average molecular weights of 465,000 g mol^{-1} (PS465k) and 206,000 g mol^{-1} (PS206k) were used in this study. PS206k and PS465k were purchased from Brunschwing (Basel, Switzerland) and Polysciences, Inc. (Warrington, PA, USA). Their characteristics, as determined by GPC, are summarized in Table 1.

The polymers, were delivered in powder form and were kept for several weeks at 70 °C under vacuum before usage in order to eliminate eventual residual solvent. Samples were prepared by the following procedure. The polymer powder was first pressed into tablets at room temperature. The tablets were then compression moulded under vacuum for 30 min under 22 bar at 190 and 200 °C for PS206k and PS465k. Samples for the rheo-optical elongation experiments required a smooth surface and were moulded between glass plates. Parallelepipedic specimens were machined with the following dimensions: a total length of 56 mm, a width of 10 mm, and a thickness of 1 or 0.4 mm. All samples were stored under vacuum at 70°C prior to the measurements.

Linear viscoelastic measurements

The linear viscoelastic properties of the sample were determined by small amplitude oscillatory shear-flow experiments with a UDS 200 mechanical spectrometer from Paar Physica, in parallel-plate geometry (diameter 25 mm). The storage and loss moduli were measured over a certain frequency range at 135, 140, 150, 160, and 180°C (190 °C for PS465k) under nitrogen atmosphere. Master curves at a reference temperature of 150 °C were obtained, via the time–temperature superposition principle, using both vertical and horizontal shift factors. The horizontal shift factors were found to follow the WLF equation (Ferry 1980) with ${c_1}^0 = 6.8$ and ${c_2}^0 = 98$ for T_0 = 150 °C.

Table 1 Characteristics of the polystyrenes as determined by GPC

Polymer	M_w (g mol^{-1})	M_n (g mol^{-1})	$I = M_w/M_n$
PS206k	206,000	198,000	1.04
PS465k	465,000	430,000	1.08

Stress and birefringence measurements

Experimental set-up and procedure

The simultaneous stress and birefringence measurements have been performed using the set-up described in Venerus et al. (1999). It consists of a Meissner-type metal belt rheometer RME (Meissner and Hostettler 1994) which has been modified to measure flow birefringence. The sample is held between two pairs of rotating metal belt clamps and supported by a nitrogen cushion. Constant speed rotation of the belts imposed a uniaxial deformation of the sample at constant strain rate. The force $F(t)$ required to stretch the sample is measured with a sensitive leaf spring attached to one of the clamps. The tensile stress is then given by:

$$\sigma(t) = \frac{F(t)}{W(t)\mathrm{d}(t)} \tag{1}$$

where $W(t)$ and $\mathrm{d}(t)$ are the time (t)-dependent width and thickness of the sample at the measuring temperature. For the flow birefringence measurements, the beam of a HeNe laser ($\lambda_{\mathrm{HeNe}} = 632.8$ nm) is directed normal to the surface of the sample and linearly polarized at 45° with respect to the flow direction. At the sample exit, a 50/50 non-polarizing beam-splitter (BS) splits the beam into two parts. One beam from the BS goes through a second polarizer oriented at −45° with respect to the flow direction and its intensity is recorded by a photodiode D1. The second beam generated by the BS passes directly to a second photodiode D2 and serves to monitor fluctuations in the transmitted intensity due to scatterin/reflection at the surface of the sample. As described in detail in Venerus et al. (1999), the ratio of the two output voltages V_1 and V_2, associated with the photocurrents delivered by the photodiodes D1 and D2, is related to the retardance $\delta(t)$ introduced by the sample via:

$$\frac{V_1(t)}{V_2(t)} = \frac{K}{2}[1 - \cos\delta(t)]. \tag{2}$$

K is a calibration factor depending on the fraction of the beam passing through the BS and the characteristics of the two intensity detection systems. Its value is determined by measuring the output voltages without the sample, and with the two polarizers oriented parallel to each other.

The birefringence of the sample is then given by:

$$\Delta n(t) = \lambda_{\mathrm{HeNe}} \frac{\delta(t)}{2\pi\mathrm{d}(t)} \tag{3}$$

where $\mathrm{d}(t)$ is the thickness of the sample.

It should be noted that the cross-polarizers system used here gives access only to the absolute value of the birefringence. The latter is negative for PS stretched above the glass transition temperature (Janeschitz-Kriegl 1983).

Compared to the original set-up of Venerus et al. (1999), a stiffer leaf spring has been mounted, extending the maximal measurable force to 250 g. A boroscope connected to a digital camera has been incorporated in the RME housing and positioned near the sample, at an angle to the laser beam, such that it does not block the laser beam. Visualisation of the middle part of the sample allowed us to check if the laser beam was passing entirely through the sample during the whole test. In addition, measurement of the variation of sample width with time allowed us to check the consistency of the strain rate and detect eventual inhomogeneous deformation.

Experiments were conducted at 140 and 150 °C for PS206k, and at 150 °C and 160 °C for PS465k. The strain rate was varied between 0.1 s^{-1} and 1 s^{-1}. Sample failure or inhomogeneous deformation limited the maximum Hencky strain to the range 3–3.5.

We note that shortly before failure, a systematic whitening of the samples was observed, which we attribute to the formation of crazes or micro-voids in the sample. Whitening was not observed for technical PS melts stretched under similar conditions.

Data evaluation and experimental errors

The tensile stress and birefringence were calculated from the initial dimensions of the sample, using Eqs. 1, 2, and 3, assuming that the deformation took place at constant strain rate and volume:

$$\frac{d(t)}{d_0} = \frac{W(t)}{W_0} = \exp\left[-\frac{\dot{\varepsilon}}{2}t\right]. \tag{4}$$

The force was calibrated with a set of weights before each measurement. The spring response was checked to be linear in the range 1–240 g. For each temperature, the same force calibration constant value was used for all measurements. The maximal error in the measured force was estimated to be 2.5%.

Measurements of the time variation of the sample width have shown that the set and true strain rate values are consistent within 3%, in agreement with independent particle tracking measurements. Data were disregarded as soon as inhomogeneous deformation was suspected.

In practice, an instantaneous constant strain rate deformation of the sample, as assumed in Eq. 4, is difficult to realize. Sagging of the sample, delayed motor response, and transducer compliance lead to a deviation from constant strain rate at the beginning of the test. This "imperfect start-up" can be detected on the calculated transient growth of the viscosity, as a departure at small strains from the linear viscoelastic response (Meissner and Hostettler 1994).

Neglecting the error in the initial dimensions of the sample, the relative error in the stress was then estimated from:

$$\frac{\Delta\sigma}{\sigma} = \frac{\Delta F}{F} + \Delta\varepsilon \text{ with } \Delta\varepsilon = \frac{\Delta\dot{\varepsilon}}{\dot{\varepsilon}}\varepsilon + \Delta\varepsilon_{\mathrm{i}} \quad (5)$$

where $\Delta\varepsilon_{\mathrm{i}} \approx 0.025$ is the estimated error in the strain involved by the imperfect start-up response of the system. According to this analysis, the error in the stress ranges from 5 to 15% for a Hencky strain of 3.

Assuming that the major source of error in the birefringence values stems from the uncertainty in the thickness of the sample, one obtains: $\Delta(\Delta n)/(\Delta n) = 1/2\Delta\varepsilon$. This error reaches 6% for a Hencky strain of 3.

We note that beyond the "imperfect" start-up period, the time-dependent relative error in the stress-optical coefficient (SOC), $C(t) = \Delta n(t)/\sigma(t)$ reduces to the time-dependent relative error in the sample width and therefore remains below 5% for a Hencky strain of 3.

Results and discussion

Linear viscoelastic properties and estimation of the Rouse time

The master curves of the dynamic moduli versus frequency of PS206k and PS465k are shown in Fig. 1 at a reference temperature of 150 °C. The zero-shear viscosity, the steady-state recoverable compliance, and weight-average terminal relaxation time were estimated according to the following relations (Ferry 1980; Graessley 1974):

$$\eta_0 = \lim_{\omega\to 0}\frac{G''(\omega)}{\omega},\ J_e^0 = \lim_{\omega\to 0}\frac{G'(\omega)}{G''(\omega)^2} \quad \text{and} \quad \tau_w = \eta_0 J_e^0$$

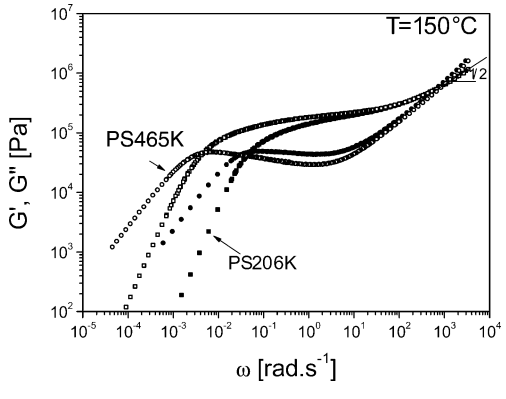

Fig. 1 Master curve of the dynamic shear moduli of PS206k (*full symbols*) and PS465k (*open symbols*) at a reference temperature of 150 °C

Two methods were used to estimate the Rouse time τ_R governing the stretch relaxation of the chains from the linear viscoelastic data (Osaki et al. 2001). τ_R is given by:

$$\tau_R = \left(\frac{\xi_0 b^2 N^2}{3\pi^2 k_{\mathrm{B}} T}\right) \quad (6)$$

where N is the number of monomers, ξ_0 is the monomeric friction coefficient, and b is the root-mean-square end-to-end distance per square root of the number of monomer units. Note that this Rouse time τ_R, characterizing chain length equilibration, is a factor two larger than the longest stress relaxation time of the Rouse model (Larson et al. 2003).

A first estimation of τ_R was obtained from the zero-shear viscosity of the melt η_0 and M_{c} the critical molecular weight for entanglement via (Menezes et al. 1982) [1]:

$$\tau_R = \frac{12 M \eta_0}{\pi^2 \rho R T}\left(\frac{M_{\mathrm{c}}}{M}\right)^{2.4},$$

where M_{c} was taken to be equal to 35,000 g mol^{-1} for PS (Ferry 1980; Majeste et al. 1998).

The second estimation was based on the variation of the storage modulus in the high frequency end of the rubbery plateau zone (Osaki et al. 2001). Over a limited frequency range, the storage modulus varies as $G'(\omega) = A\omega^{1/2}$, where A, according to the Rouse theory for non-entangled melts (Doi and Edwards 1986), is given by:

$$A = \frac{\rho R T \pi}{2\sqrt{2}M}\left(\frac{\tau_R}{2}\right)^{1/2}.$$

The evaluated quantities are summarized in Table 2. For both the PS melts, a good agreement is obtained between the Rouse time values evaluated from the zero-shear viscosity (τ_R^{η}) and from the storage modulus ($\tau_R^{G'}$). The average values, 9.6 s for PS465k and 2.4 s for PS206k, and the experimental shift factors were used to estimate the Rouse time of the melts at a given temperature.

Transient and steady mechanical data/comparison with previous results

Figures 2 and 3 show the "transient elongational viscosities" $\eta^+(t) = \sigma(t)/\dot{\varepsilon}$ obtained for PS206k at 140 and 150 °C. Transient mechanical data collected for PS465k are plotted in Fig. 4 ($T = 150$ °C) and Fig. 5 ($T =$

[1] In the original article, the expression is given for the longest stress relaxation time of the Rouse model whose value is half the value of τ_R

Table 2 Characteristic time scales for the studied polystyrenes at a temperature $T = 150$ °C

Polymer	η_0 (Pa s)	J_e^0 (Pa^{-1})	τ_w (s)	A (Pa $s^{1/2}$)	$\tau_R^{G'}$ [a] (s)	τ_R^{η} [a] (s)
PS206K	$2.33 \cdot 10^6$	$1.3 \cdot 10^{-5}$	30	$2.07 \cdot 10^4$	2.38	2.35
PS465K	$2.70 \cdot 10^7$	$1.5 \cdot 10^{-5}$	400	$2.00 \cdot 10^4$	10.55	8.74

[a] For the Rouse time evaluations, weight average molecular weights were used; the density was taken equal to 1 g cm^{-3} and M_c to 35 kg mol^{-1}

160 °C). For each strain rate, data for two or three repeated tests are shown to give an indication about the reproducibility.

All plots include the linear viscoelastic prediction $3\eta^0(t)$deduced from the complex dynamic moduli.

Except for the short imperfect start-up period, the qualitative behaviour is similar to that reported by Bach et al. (2003) for PS melts with narrow MWD. The transient viscosity first follows and then rises above the linear viscoelastic predictions. At a later time, it saturates approaching a limiting value that is below $3\eta_0$. As noticed by Schweizer (2000), this last regime where the tensile stress attains a constant value corresponds to a "highly unstable situation for the sample and the faintest irregularity in the cross-section leads immediately to necking and rupture". Control of neck location and of the strain rate within the neck region is a major advantage of the filament stretching technique used by Bach et al. (2003) and allowed them to obtain a steady state of over 1 to 2 Hencky strain units. In our case, a regime of constant tensile stress could be observed only within a very narrow time window, allowing us to extract only estimates of the steady-state stress or viscosity.

Estimated "steady-state" stress values for PS206k and PS465K are reported versus the Rouse time-based Deborah number$De_R = \dot{\varepsilon}\tau_R$, where τ_R denotes the Rouse

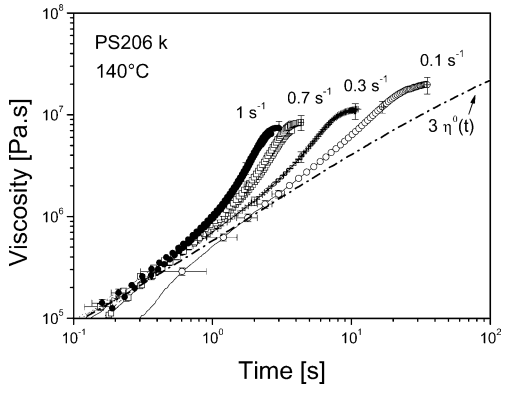

Fig. 2 Transient uniaxial elongational viscosity versus time during the elongation at constant strain rate of PS206k at 140 °C. The dash-dotted line represents the linear viscoelastic response deduced from the dynamic shear moduli

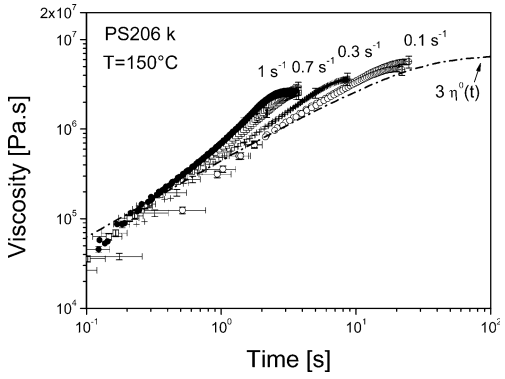

Fig. 3 Same as Fig. 2 for PS206k at 150 °C

time characterizing chain length equilibration (see Eq. 6), in Fig.6.

For the purpose of comparison, the figure includes steady-state data extracted from previous investigations on quasi-monodisperse PS melts: the study of Li et al. (1988) and the study by Bach et al. (2003). For all literature data sets, Rouse time was estimated, as described in the previous section, from the reported weight average molecular weight and zero-shear viscosity values. To illustrate typical predictions of reptation-based models including chain stretch and finite extensibility, simulation results of the model of Öttinger (1999) are shown for three different $Z = \tau_d/3\tau_R$ ratios. τ_d and τ_R are the chain reptation and Rouse time, the other model parameters, maximum stretch λ_{max} and plateau modulus G_N^0, being set to values that are appropriate for PS melts: $\lambda_{max} = 4.5$, $G_N^0 = 170$ kPa (for more details see Fang et al. 2000; van Meerveld 2004a).

The following points can be underlined. The model predictions for different $\tau_d/3\tau_R$ values, e.g., different molecular weights, fall onto a unique curve for $De_R > 1$. As soon as chain stretch sets in ($De_R > 1$), the rate dependence of the steady-state stress shows a steep increase that corresponds to the up-turn in the steady-state

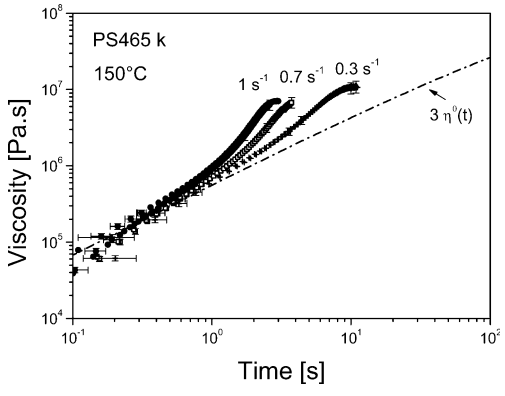

Fig. 4 Same as Fig. 2 for PS465k at 150 °C

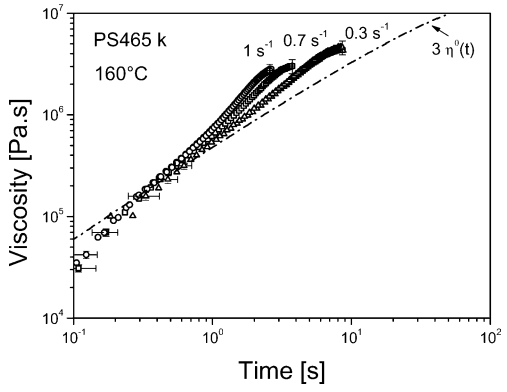

Fig. 5 Same as Fig. 2 for PS465k at 160 °C

viscosity, mentioned in the introduction. Although they cannot be considered as a validation, our estimated steady-state mechanical data for PS206k and PS465k, appear to be in close agreement with that of Bach et al. (2003). They do not reveal any abrupt change in the rate dependence of the steady-state stress in the vicinity of $De_R \approx 1$, in contrast to the trend shown by the early data of Li et al. (1988), and to the current model predictions. Within the whole investigated range, the steady-state stress scales approximately as $\sigma_{ss} \propto (De_R)^{\alpha}$ with $\alpha \approx 0.6 \pm 0.1$. In the next section, we will show that this scaling, that corresponds to a continuous decrease of the steady elongational viscosity with the strain rate, is observed even in the regime where the stress-optical rule is violated, e.g., where significant chain stretching is present.

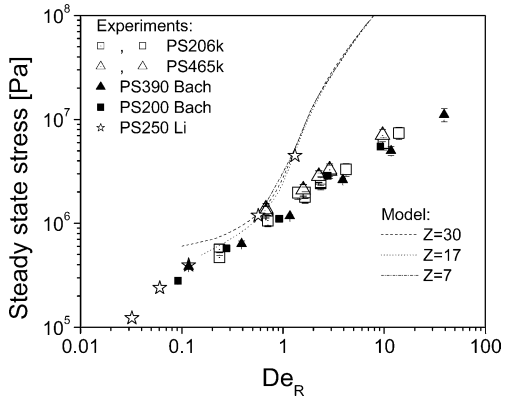

Fig. 6 Steady-state stress versus the Rouse time-based Deborah number $De_R = \dot{\varepsilon}\tau_R$: experimental data obtained in this work for PS206K (⊡ : 150 °C; □: 140 °C) and PS465k (*dotted triangle*: 150 °C; △: 160 °C); data by Bach extracted from Figs. 4 and 5 of Bach et al. (2003) for two PS melts with $M_w = 200$ kg mol^{-1} ($M_w/M_n = 1.04$, $\eta_0 = 84$ MPa s at 130 °C) and $M_w = 390$ kg mol^{-1} ($M_w/M_n = 1.06$, $\eta_0 = 755$ MPa s at 130 °C); data by Li extracted from Fig. 8 of Li et al. (1988) for a PS melt with $M_w = 250$ kg mol^{-1} ($M_w / M_n = 1.15$, $\eta_0 = 0.93$ MPa s at 160 °C). Lines represent simulation results from the model studied in Fang et al. (2000) for three different values of $Z = \tau_d/(3\tau_R)$

Stress-optical behavior

To analyse the stress-optical behaviour and determine the regime of validity of the SOR, time-dependent birefringence data are plotted directly as function of tensile stress.

Figure 7 (a–b) illustrates the response measured for PS206k at 150 °C for two different elongation rates. For an elongation rate of 0.3 s^{-1} (Fig. 7a), birefringence varies linearly with the tensile stress. The slope corresponds to a SOC equal to $|C_0| = (4.6 \pm 0.1) \cdot \times 10^{-9}$Pa^{-1} that is in agreement with the reported values between 4 and 5×10 $^{-9}$ Pa^{-1} for PS melts (Janeschitz-Kriegl 1983). From the inset, representing the corresponding time-variation of stress and birefringence, one can see that data were collected upto the steady state. Therefore at this rate, equivalent to a Rouse time-based Deborah number of about 0.7, the SOR is valid upto the steady state, indicating that whenever chain stretch occurs it remains within the Gaussian regime.

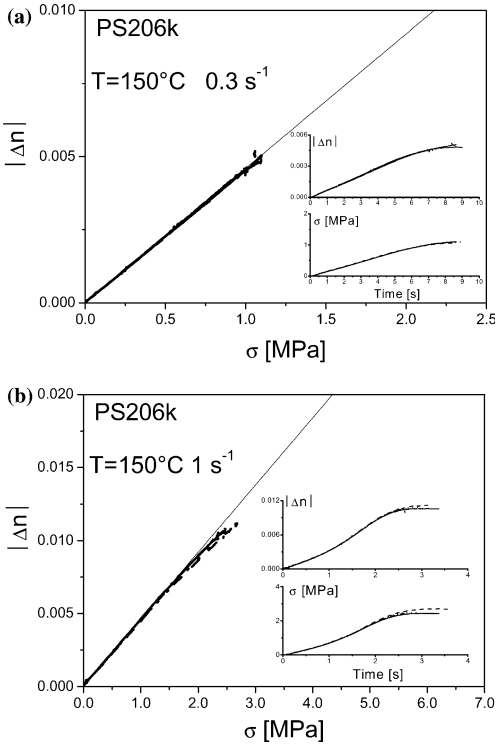

Fig. 7 Absolute value of the flow-induced birefringence versus tensile stress for PS206k at 150 °C. The slope of the thin line corresponds to a SOC $|C| = 4.6\ 10^{-9}$ Pa^{-1} . The inset shows the corresponding time evolution of the birefringence (*top*) and the tensile stress (*bottom*). **(a)** Three repeated elongation tests at a constant strain rate of 0.3 s^{-1} . **(b)** Four repeated tests at 1 s^{-1}

Increasing the strain rate to 1 s^{-1}, e.g.$De_R \approx 2.4$, small departures from linearity appear at large stresses (see Fig. 7b). Though systematic, the observed decrease in the apparent SOC $C(\sigma) = \Delta n(t)/\sigma(t)$ only slightly exceeds the estimated experimental error of 5% at the steady state.

Figure 8 presents the birefringence versus tensile stress for the four investigated elongational rates when the temperature is lowered to 140 °C. At this temperature, a strong downwards departure from linearity is evidenced in the high-stress region that can be reached at strain rates of 0.7 and 1 s^{-1}. This clear failure of the SOR is in accordance with previous observations on polydisperse PS melts (Matsumoto and Bogue 1977; Muller and Froelich 1985; Muller and Pesce 1994; Venerus et al. 1999). It corresponds to a decrease of the apparent SOC (upto 25% for 1 s^{-1}) and is consistent with the occurrence of significant chain stretching. We believe that the apparent increase of the SOC at large deformation observed by Kotaka et al. (1987) for a melt with a relatively narrow MWD is due to necking within the optically probed sample region (overestimation of the actual sample width).

Data collected for different strain rates appear to fall into a unique curve indicating that the stress-optical behaviour is essentially independent of the elongational rate even in the nonlinear region. The same observation was previously made by Muller and Froelich in 1985 and by Muller and Pesce in 1994 on polydisperse PS melts stretched at relatively low temperatures (120–130 °C). In the low-stress region, all data follow a straight line consistent with the SOC value obtained at 150 °C $|C_0| = (4.6 \pm 0.1) \cdot 10^{-9}\,\mathrm{Pa}^{-1}$.

Figure 9 shows that similar conclusions can be drawn from the data collected on PS465k. In addition it shows that the relationship between tensile stress and birefringence is basically the same for both molecular weights.

In order to assess the onset of failure of the SOR quantitatively, we use, as a criterion, a 5% decrease in the apparent SOC. According to this criterion, the SOR fails, for both PS melts with NMWD, above a critical stress level $\sigma_{c5\%} = (2.7 \pm 0.5)$ MPa. Ten percent deviation is reached for a stress level $\sigma_{c10\%} = (3.7 \pm 0.5)$ MPa. Compared to polydisperse melts, these values are relatively close to the 2 MPa reported in the studies of Muller and Froelich (1985) and Muller and Pesce (1994) but are definitely larger than the 0.5–1 MPa obtained by Venerus et al. (1999). These differences in critical stresses are reminiscent of polydispersity effects on the limit of validity of the SOR (van Meerveld 2004b). Table 3 summarizes the tests performed on both melts and the validity/non-validity of the SOR, again based on a criterion of 5% deviation. It indicates that, the SOR is violated at the steady state when De_R exceeds a value of about 3. Reporting these values in Fig. 6, one can see that, in terms of either stress levels or Rouse time-based Deborah numbers, the regime of extensional thinning observed by Bach et al. (2003) extends well beyond the onset of failure of SOR and therefore the onset of significant chain stretching.

Concerning the degree of chain stretching, one can notice in Fig. 9 that the birefringence does not show any sign of saturation at large stresses, suggesting that in the regime investigated here, the chains did not reach their full extension. The maximum birefringence reached, of about −0.025 at a stress of 7 MPa, remains significantly smaller than the maximal birefringence that is expected when the PS chains are fully extended. For the latter, a value close to −0.1 (Jasse and Koenig 1979; Neuert et al. 1985) is inferred from the combination of birefringence with, eg., IR-dichroism measurements that give access to the second moment of the orientational distribution of the polymer segments, under the assumption that the transition dipole moment associated with the vibration

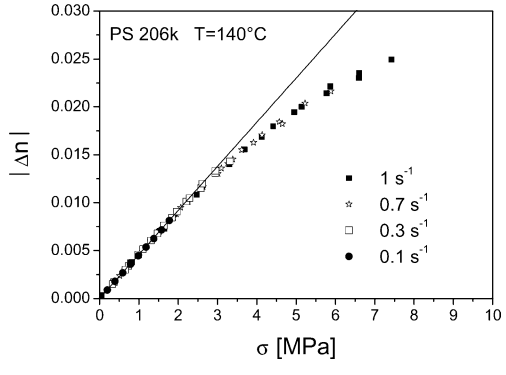

Fig. 8 Absolute value of birefringence versus stress for PS206k during elongation at 140 °C for four different strain rates. The slope of the thin line corresponds to a SOC $|C| = 4.6\ 10^{-9}\ \mathrm{Pa}^{-1}$

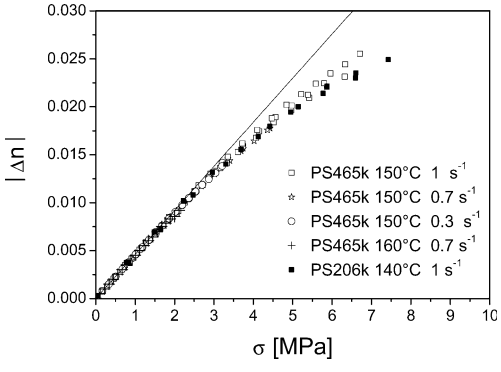

Fig. 9 Absolute birefringence value versus tensile stress for PS465k during elongation at constant strain rate. The filled square symbols recall the response measured for PS206k at 140 °C and a strain rate of $1 s^{-1}$. The slope of the thin line corresponds to a stress-optical coefficient $|C| = 4.6\ 10^{-9}\ \mathrm{Pa}^{-1}$

Table 3 Summary of the tests performed and occurrence of deviations from the SOR, based on a criterion of 5% deviations

Sample	T (°C)	$\dot{\varepsilon}(s^{-1})$	$\dot{\varepsilon}\tau_R$	Deviation SOR
PS206k	150	0.1	0.24	$<$ 5%
PS206k	150	0.3	0.71	$<$ 5%
PS206k	150	0.7	1.7	$<$ 5%
PS206k	150	1	2.4	$\sim$ 5%
PS206k	140	0.1	1.4	$<$5%
PS206k	140	0.3	4.2	$\sim$ 5%
PS206k	140	0.7	9.8	$\gg$ 5%
PS206k	140	1	14	$\gg$ 5%
PS465k	160	0.3	0.7	$<$ 5%
PS465k	160	0.7	1.6	$\sim$ 5%
PS465k	160	1	2.3	$\sim$ 5%
PS465k	150	0.3	2.9	$\sim$ 5%
PS465k	150	0.7	6.8	$\gg$ 5% [a]
PS465k	150	1	9.6	$\gg$ 5%

[a]For these tests the "steady-state" has not been reached

mode under consideration makes a specific angle with the chain axis (see Ward 1975). It cannot be excluded that the actual maximum birefringence of the melt is limited to a lower value, either due to an actual saturation as a function of stress, or due to systematic sample failure. This issue could not be addressed here, since our limited measurable force range did not allow us to investigate the stress-optical behaviour for larger Deborah numbers.

Summary and conclusions

Simultaneous measurements of tensile stress and flow-induced birefringence have been carried out during the uniaxial elongation at constant strain rate of two PS melts with a NMWD. The investigated temperature/strain-rate range corresponds to a variation of the Rouse time-based Deborah number from approximately 1 to 10. Inhomogeneous sample deformation and sample rupture limited the maximum reachable Hencky strain within 3–3.5 and thereby the possibility to extract accurate steady-state data. Approximate steady-state values were found, however, to be in good correspondence with the recent mechanical data obtained by Bach et al. (2003) on similar systems with a filament stretching rheometer, and in particular consistent, within the whole investigated Deborah number range, with the reported continuous decrease of steady-state viscosity with strain rate. For both melts, the SOR was shown to be valid upto a critical stress level of 2.7 ± 0.5 MPa. Above this stress level, which can be reached for a Rouse time-based-Deborah number De_R of about 3, departure from linearity occurs, which corresponds to a decrease of the apparent SOC. The detected decrease of the SOC attains 25% for the largest De_R explored in this study and provides a clear experimental signature of a significant chain stretch beyond the Gaussian regime.

The following conclusions can be drawn:

1. The continuous decrease of the steady elongational viscosity with the strain rate, evidenced by Bach et al. (2003), extends well beyond the onset of failure of the SOR, and therefore the onset of chain stretch in the non-Gaussian regime.
2. The one-to-one relationship between the tensile stress and the birefringence confirms the picture that, in this regime, the stress can be determined knowing the stretch and orientation of the chains. This of course is not valid for extremely large Rouse time-based Deborah numbers, where phenomena related to the glass transition may occur.
3. The question whether chains reach their maximal extension could not be answered definitively. The absence of birefringence saturation at large stresses as well as the maximum birefringence level reached indicates that at least upto a stress level of about 7 MPa, chains do not reach full extension.

Acknowledgements The authors are grateful to Martin Colussi for performing the GPC measurements, to Marina Karlina, Werner Schmidheiny, and Fredy Mettler for their assistance in conducting the experiments. Clarisse Luap thanks Martin Kröger and Jan van Meerveld for helpful discussions.

References

Bach A, Almdal K, Rasmussen HK, Hassager O (2003) Elongational viscosity of narrow molar mass distribution polystyrene. Macromolecules 36:5174–5179

Bhattacharjee PK, Oberhauser JP, McKinley GH, Leal LG, Sridhar T (2002) Extensional rheometry of entangled solutions. Macromolecules 35:10131–10148

Doi M, Edwards SF (1986) The theory of polymer dynamics. Oxford Science, New York

Fang J, Kröger M, Öttinger HC (2000) A thermodynamically admissible reptation model for fast flows of entangled polymers. II. Model predictions for shear and extensional flows. J Rheol 44:1293–1317

Ferry JD (1980) Viscoelastic properties of polymers, 3rd ed. Wiley, New York

Graessley WW (1974) The entanglement concept in polymer rheology. Adv Polym Sci 16:1–179

Janeschitz-Kriegl H (1983) Polymer melt rheology and flow birefringence. Springer, Berlin Heidelberg New York

Jasse B, Koenig JL (1979) Fourier transform infrared study of uniaxially oriented atactic polystyrene. J Polym Sci Polym Phys Ed 17:799–810

Kotaka T, Kojima A, Okamoto M (1997) Elongational flow opto-rheometry for polymer melts. 1. Construction of an elongational flow opto-rheometer and some preliminary results. Rheol Acta 36:646–656

Larson RG, Sridhar T, Leal LG, McKinley GH, Likhtman AE, McLeish TCB (2003) Definitions of entanglement spacing and time constants in the tube model. J Rheol 47:809–818

Li L, Masuda T, Takahashi M, Ohno H (1988) Elongational viscosity measurements on polymer melts by a Meissner-type rheometer. J Soc Rheol Jpn 16:117–124

Majeste JC, Montford JP, Allal A, Marin G (1998) Viscoelasticity of low molecular weight polymers and the transition to the entangled regime. Rheol Acta 37:486–499

Marrucci G, Grizzuti N (1988) Fast flows of concentrated polymers: Predictions of the tube model on chain stretching. Gazz Chim Italiana 118:179–185

Marrucci G, Ianniruberto G (2004) Interchain pressure effect in extensional flows of entangled polymer melts. Macromolecules 37:3934–3942

Matsumoto T, Bogue DC (1977) Stress birefringence in amorphous polymer under nonisothermal conditions. J Polym Sci Polym Phys Ed 15:1663–1674

Mead DW, Leal LG (1995) The reptation model with segmental stretch. I) Basic equations and general properties. Rheol Acta 34:339–359

van Meerveld J (2004a) Modified constraint release in molecular based reptation models for fast flows. J non-Newtonian Fluid Mech 122: 263–272

van Meerveld J (2004b) Validity of the linear stress optical rule in mono-, bi- and polydisperse systems of entangled linear chains. J non-Newtonian Fluid Mech 123: 259–267

Meissner J, Hostettler J (1994) A new elongational rheometer for polymer melts and other highly viscoelastic liquids. Rheol Acta 33:1–21

Menezes EV, Graessley WW (1982) Nonlinear rheological behavior of polymer systems for several shear-flow histories. J Polym Sci Polym Phys Ed 20:1817–1833

Muller R, Froelich D (1985) New extensional rheometer for elongational viscosity and flow birefringence measurements: some results on polystyrene melts. Polymer 26:1477–1482

Muller R, Pesce JJ (1994) Stress-optical behavior near the Tg and melt flow-induced anisotropy in amorphous polymers. Polymer 35:734–739

Neuert R, Springer H, Hinrichsen G (1985) Orientation analysis of uniaxially drawn polystyrene films doped with fluorescent molecules by fluorescence polarization, UV- and IR-dichroism and birefringence. Colloid Polym Sci 263:392–395

Osaki K, Inoue T, Eumatsu T, Yamashita Y (2001) Evaluation methods of the longuest rouse relaxation time of an entangled polymer in a semidilute solution. J Polym Sci Part B Polym Phys 39:1704–1712

Öttinger HC (1999) A thermodynamically admissible reptation model for fast flows of entangled polymers. J Rheol 43:1461–1493

Schweizer T (2000) The uniaxial elongational rheometer RME—six years of experience. Rheol Acta 39:428–443

Takahashi M, Isaki T, Takigawa T, Masuda T (1993) Measurement of biaxial and uniaxial extensional flow behavior of polymer melts at constant strain rates. J Rheol 37:827–846

Venerus DC, Zhu S-H, Öttinger HC (1999) Stress and birefringence measurements during the uniaxial elongation of polystyrene melts. J Rheol 43:795–813

Ward IM (1975) Structure and properties of oriented polymers. Applied Science Publishers, London

Ye X, Larson RG, Pattamaprom C, Sridhar T (2003) Extensional properties of monodisperse and bidisperse polystyrene solutions. J Rheol 47:443–468